

Phthalocyanine–titanate nanotubes: a promising nanocarrier detectable by optical imaging in the so-called imaging window

Jérémy Paris, Yann Bernhard, Julien Boudon, Olivier Heintz, Nadine Millot, Richard A. Decréau

▶ **To cite this version:**

Jérémy Paris, Yann Bernhard, Julien Boudon, Olivier Heintz, Nadine Millot, et al.. Phthalocyanine–titanate nanotubes: a promising nanocarrier detectable by optical imaging in the so-called imaging window. RSC Advances, 2014, 5 (9), pp.6315-6322. 10.1039/c4ra13988g . hal-03263264

HAL Id: hal-03263264
https://hal.science/hal-03263264

Submitted on 19 Oct 2022

HAL is a multi-disciplinary open access archive for the deposit and dissemination of scientific research documents, whether they are published or not. The documents may come from teaching and research institutions in France or abroad, or from public or private research centers.

L'archive ouverte pluridisciplinaire **HAL**, est destinée au dépôt et à la diffusion de documents scientifiques de niveau recherche, publiés ou non, émanant des établissements d'enseignement et de recherche français ou étrangers, des laboratoires publics ou privés.



Distributed under a Creative Commons Attribution - NonCommercial 4.0 International License

RSC Advances



This is an *Accepted Manuscript*, which has been through the Royal Society of Chemistry peer review process and has been accepted for publication.

Accepted Manuscripts are published online shortly after acceptance, before technical editing, formatting and proof reading. Using this free service, authors can make their results available to the community, in citable form, before we publish the edited article. This *Accepted Manuscript* will be replaced by the edited, formatted and paginated article as soon as this is available.

You can find more information about *Accepted Manuscripts* in the Information for Authors.

Please note that technical editing may introduce minor changes to the text and/or graphics, which may alter content. The journal's standard Terms & Conditions and the Ethical guidelines still apply. In no event shall the Royal Society of Chemistry be held responsible for any errors or omissions in this *Accepted Manuscript* or any consequences arising from the use of any information it contains.

ROYAL SOCIETY OF CHEMISTRY

www.rsc.org/advances

Journal Name

RSCPublishing

ARTICLE

Phthalocyanine-Titanate Nanotubes: a promising nanocarrier detectable by optical imaging in the so-called imaging window

Cite this: DOI: 10.1039/x0xx00000x

J. Paris,[a] Y. Bernhard,[b] J. Boudon,[a] O. Heintz,[a] N. Millot*[a] and R. A. Decréau*[b]

Received 00th January 2012,
Accepted 00th January 2012

DOI: 10.1039/x0xx00000x

www.rsc.org/

TiONts-phthalocyanine nanohybrids combining an efficient optical probe and a promising nanovector have been developed in a *step-by-step* approach and were thoroughly characterized. Each 150-nm long TiONts–Pc bear *ca*. 450 Pc. Three nanohybrids were prepared including three different linkers in quest for the best stability.

Introduction

Various techniques are used to diagnose diseases at an early stage of their developments, such as radiography, tomography (CT, PET, SPECT),[1, 2] Magnetic Resonance Imaging (MRI).[3] Optical Imaging (OI) is used in ophthalmology, but is also mostly used in preclinical studies.[4] Two aspects are crucial in imaging, the contrast agent and the nature of the delivery system. Our study focuses on optical imaging probes and tube-shaped nanoparticles to deliver them. The immobilization of OI probes on nanotubes has been reported many times in the case of carbon nanotubes (CNT) and showed great potential,[5] but their design did not address either of the following issues: (a) exploring new types of nanotubes (not only carbon-based); (b) the robustness of fluorophores, *i.e.* the sensitivity to photobleaching; (c) the construction of optically active nanohybrids was not achieved *step-by-step*, hence the precise composition of coating/nanotube may not be accurate enough; (d) the fluorophore/nanotube carrier may not necessarily unravel a potency for therapeutic applications.

Hence, we envisioned that conjugates **1a-c** (Fig. 1) might address these issues:

(a) most nanotubes used so far for the immobilization of OI probes are CNT.[5] Titanate nanotubes (TiONts) have been recently presented, hence they remain barely studied for biomedical applications.[6-8] They are needle-shaped nanocarriers, with a 10 nm outer diameter, 4 nm inner diameter. Contrary to CNT, they are opened on the extremities. They have been reported as carriers for polyethylene imine (PEI) in *in vitro* studies for DNA transfection[7] and as radiosensitizer of glioma.[8]

(b) Zinc phthalocyanines (ZnPc) are robust fluorophores (and also photosensitizers, which does not prevent their use as fluorescent probes), with appealing optical properties:[9-11] i) absorption/emission bands in the 650–800 nm region lies in the wavelength range where the tissue penetration is the greatest (*i.e.* the so-called imaging window);[9-11] ii) a fluorescence quantum yield (ΦF (ZnPc) = 0.3) in the range of known fluorophores,[9-11] and a high molar extinction coefficient (ε = 10^5 $M^{-1}.cm^{-1}$), which results in a high brightness (ε × Φ_F) and making ZnPc very competitive compared to other near–IR emitting fluorophores (for example ZnPc is already used in clinics).[9-11] Moreover, ZnPc is one of the most robust photobleaching-resistant fluorophores reported to date, with degradation quantum yield of 10^{-6}, *i.e.* about 30 times more robust than rhodamine. Eventually it can be combined to inorganic structures to form hybrid materials of interest particularly for chemosensing.[12]

(c) An organic coating was covalently attached onto TiONts in a *step-by-step* approach.

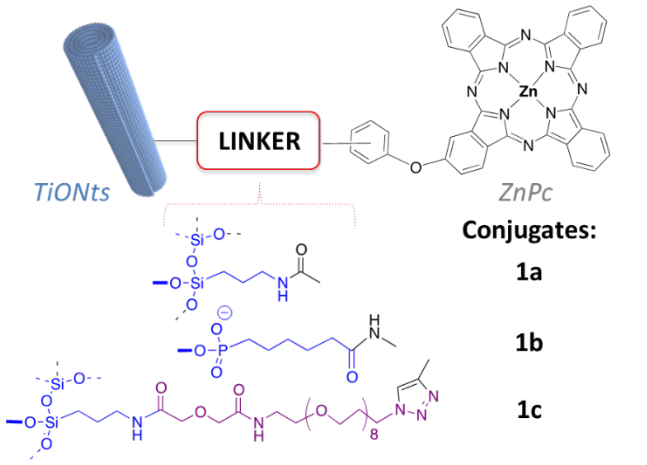


Fig. 1 Three TiONts-Pc conjugates: three linkers.

Results and discussion

Each coated-TiONts was thoroughly characterized by an array of analytical techniques, which allowed us to keep track of the

RSC Advances Accepted Manuscript

precise composition of the coated-TiONts at a given step. We stuck to the highest standards of characterization on hybrid materials.[13-17] (d) ZnPc are used in photodynamic therapy (PDT), whereas TiONts are used as a radiosensitizers;[8] our experience in nano-objects (SuperParamagnetic Iron Oxide Nanoparticles (SPIONs) and nanotubes)[6-8, 13-15] and on the immobilization of functional porphyrin/porphyrinoid models on iron oxide and gold material,[15-18] prompted us to investigate the immobilization of ZnPc onto TiONts, two promising components featuring effective vectorization of efficient OI probes.

Three approaches have been explored to immobilize Pc onto TiONts, (featuring three Pc–Y / TiONts–X couples, Fig. 2) to examine (i) the corresponding reactivities and convenience in handling three types of linkers in conjugates **1a-c** (Fig. 1), (ii) and most importantly the colloidal stability, *i.e.* kinetics of decantation. Herein, we synthesized X-functionalized titanate nanotubes (X = COOH, NH_2, and N_3) (Fig. 2).

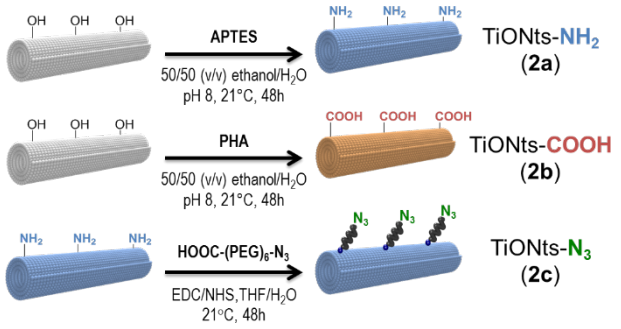


Fig. 2 Step-by-step syntheses of X–functionalized TiONts: TiONts–NH_2 (**2a**), TiONts–COOH (**2b**), TiONts–N_3 (**2c**) (for subsequent reactions with phthalocyanines **3a-c**, respectively).

Bare TiONts were prepared according to the procedure reported elsewhere.[19] The dimension of nanotubes is given by Transmission Electron Microscopy (TEM), with a length (L = 156 ± 53 nm), an outside diameter (doutside = 9.1 ± 1.3 nm) and an internal cavity (dinner = 3.8 ± 0.6 nm) (Fig. 3).

Bare TiONts were also characterized by ThermoGravimetric Analysis (TGA) and showed 4.7 OH/nm² (Fig. S5, Table S2). The specific surface area of the powder is S = (163 ± 25) $m^2.g^{-1}$. ζ-potential measurements (Fig. 4I) indicated an IsoElectric Point (IEP) at pH 3.3 and potentials that reached 35 mV at their maximum values.

TiONts–X Syntheses. Bare TiONts were coated by the reaction between TiONts free hydroxyl groups and 3-aminopropyltriethoxysilane (APTES), to afford amine-functionalized TiONts (**TiONts–NH_2**, **2a**). ζ-potential measurements (Fig. 4I) indicated an IEP at 6.5, which was shifted at a higher pH value compared to bare titanate nanotubes. The latter shift is due to the presence of amine functions at the nanotubes surface and maximum potentials are still about 35 mV. TGA suggests that the number of amine groups is about 5.5 NH_2/nm² (9.1 µmol/m²) on these TiONts–NH_2 (Fig. S5, Table S2). The XPS measurements showed that the C1s peak decomposes into two different contributions: C–C/C–H (284.5 eV, 64%), C–N (285.9 eV, 36%) (Fig. S2). The N1s peak (not shown) corresponds to two contributions: C–NH_2 (399.2 eV, 54%) and C–NH_3^+ (401.1 eV, 46%).[20] Carbon and nitrogen atomic concentrations have increased (Table S1). All these observations may be explained because of the presence of the APTES.

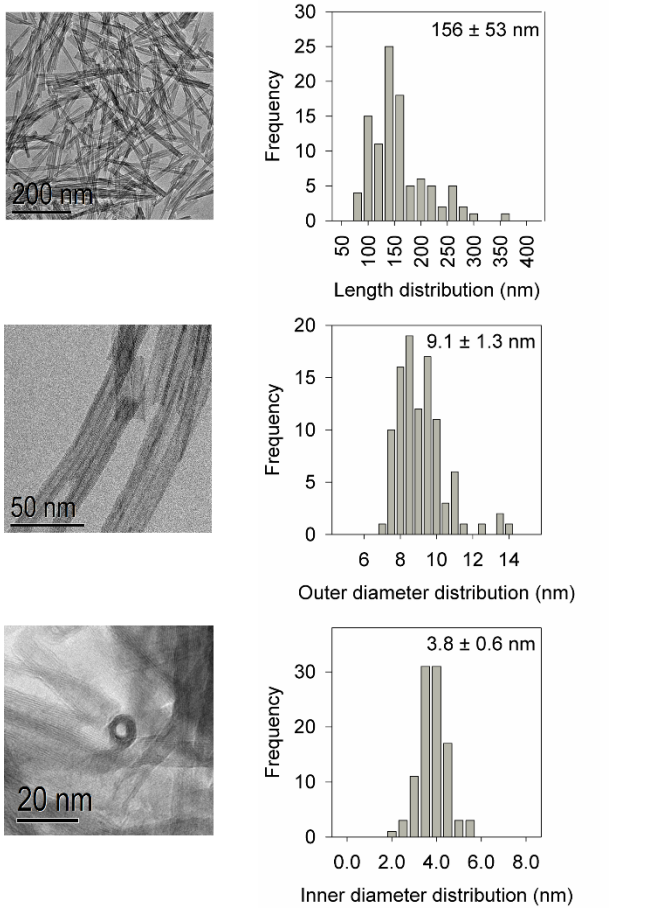


Fig. 3 TEM images of bare titanate nanotubes and distribution of length, outer and inner diameter

Another variant of functionalized TiONts, **TiONts–COOH 2b** were synthesized as follows. Bare TiONts were coated by the reaction between TiONts free hydroxyl groups and 6-phosphonohexanoic acid (PHA), to afford carboxyl-functionalized TiONts. ζ-potential measurements indicated an IEP at 3.2, shifted at a lower pH value because of the presence of carboxyl groups at the nanotubes surface. The maximum potentials are still about 35 mV when compared to bare TiONts (Fig. S2bis). TGA suggests that the number of carboxylic groups is about 3.5 COOH/nm² (5.8 µmol/m²) on these TiONts–COOH (Fig. S5, Table S2). The XPS measurements showed that the C1s peak decomposes into three different contributions: C–C/C–H (284.5 eV, 64%), C–P (286.2 eV, 26%), (C=O)–OH (288.0 eV, 10%) (Fig. S2). Carbon and

RSC Advances Accepted Manuscript

This journal is © The Royal Society of Chemistry 2012

Journal Name

RSCPublishing

ARTICLE

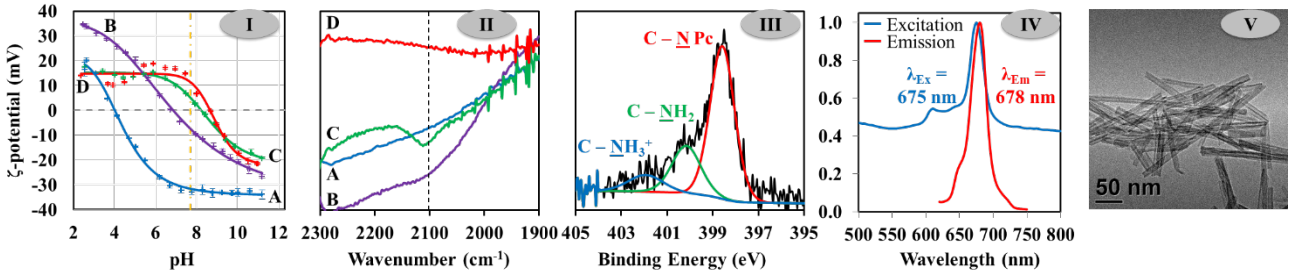


Fig. 4 Characterization of TiONts–Pc **1c** (from click coupling): (I) ζ-potential and (II) FTIR (both labeled: A: TiONts; B: TiONts–NH_2 (**2a**); C: TiONts–N_3 (**2c**); D: TiONts-Pc (**1c**); A, B and C being shown for comparison); (III) TiONts–Pc XPS contributions for nitrogen N1s; (IV) TiONts–Pc fluorescence; (V) TiONts–Pc TEM image.

phosphorus atomic concentrations have increased because of the presence of PHA (Table S1).

TiONts–NH_2 nanohybrids **2a** were subsequently coupled with heterobifunctional azide/carboxyl terminated–PEG (polyethylene glycol) chains by EDC coupling, to afford azido-functionalized TiONts (**TiONts–N_3**, **2c**). They were characterized by FTIR (Fig. 4II) exhibiting a characteristic azide stretch at 2110 cm^{-1}. ζ-potential measurements (Fig. 4I) indicated an IEP shifted up to the higher pH value of 7.9, coming along with a 20 mV decrease to a maximum potential of 15 mV. These observations are consistent with the modification of the NP surface introducing azide groups (IEP variation) at the end of short ethylene oxide chains (significant shielding effect).

XPS measurements are in correlation with the other characterizations: the C1s peak decomposes into three different contributions: C–C/C–H (284.5 eV, 38%), C–NH_2/C–OPEG–N_3/(C=O)–NH–C (286.0 eV, 48.5%), (C=O)–NH–C/C=OPEG–N_3 (287.8 eV, 13.5%) (Fig. S2). The N1s peak corresponds to C NH_2/(C=O)–NH–C (399.6 eV, 68%) and C–NH_3^+ (401.3 eV, 32%) contributions (Table S1).[21] In addition, TGA measurements (Fig. S10) indicated 0.6 PEG–N_3/nm² (1.0 µmol/m²) meaning that 1 NH_2 function over 10 reacted with HOOC–PEG(9)–N_3. All TiONts–X were also characterized by TEM (Fig. S1). Surface modifications of nanotubes **3a-c** led to small agglomerates of **2a-c**, which is in stark contrast with bare TiONts made of micrometric-sized agglomerates. These results are in agreement with previous observations of PEI modified nanotubes.[7]

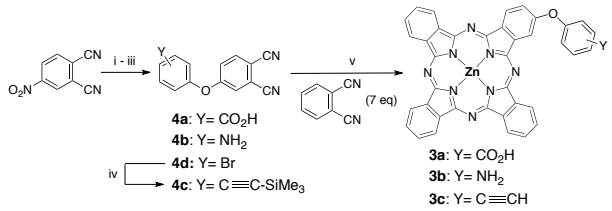
Pc–Y Syntheses. A series of phthalocyanines **3a-c** were synthesized by mixed condensation of two phthalonitriles, *i.e.* plain phthalonitrile and functionalized phthalonitrile **4a-c** (R = COOH, NH_2, alkyne) (Scheme 1). The latter were synthesized by nucleophilic aromatic substitution of nitrodicyanobenzene onto 3-hydroxy-benzoic acid (for **4a**), or 4-amino-phenol (for **4b**), or 4-bromophenol (for **4d**). Alkynyl derivative **4c** was prepared by Sonogashira coupling between **4d** and TMS-protected acetylene. The mixed condensation led to a statistical mixture containing the Y-bearing A_3B-ZnPc phthalocyanine **3a-c** and the A_4-ZnPc counterpart that is not reactive to achieve subsequent grafting onto surfaces. This mixture was purified by a series of washings (with various solvents), leading to the removal of the non-phthalocyanine material. The ratio of A3B/A4 Pcs was estimated by ^{1}H-NMR to be 4:7 (Fig. S2tris).

TiONts–Pc syntheses. Pc-modified TiONts were synthesized depending on the nature of the Y function on the Pc and according to the following procedures: nanohybrid **1a** was synthesized from the condensation of TiONts–NH_2 **2a** and Pc–COOH **3a**, whereas nanohybrid **1b** was synthesized by condensation of TiONts–COOH **2b** and Pc–NH_2 **3b**; both conjugations were carried out in the presence of EDC/NHS. Nanohybrid **1c** was synthesized by the Cu-catalyzed Azide-Alkyne Coupling (CuAAC) between the azide-containing TiONts–N_3 **2c** and the alkynyl-phthalocyanine **3c** in the presence of a copper catalyst and sodium ascorbate (AsNa). The remaining A4-ZnPc coproduct that does not bear the Y moiety (such as COOH, NH_2, alkynyl, see Fig. 4, scheme 1) is not reactive for subsequent immobilization, and hence was easily washed away after the coupling reaction with TiONts (Moreover, a series of washings with various solvents efficient at dissolving free A3B/A4 phthalocyanine was used). A mixture of ZnPc and TiONts treated without either the coupling agents (**1ab**), or the Cu catalyst (**1c**) did not lead to the characteristic spectroscopic features indicating the formation of the TiONts–Pc conjugates **1a-c**. Hence, this indicates that these spectroscopic observations, such as that of UV-Vis do not reflect an artifact such as the adsorption of ZnPc onto TiONts, but a covalent linkage instead. Note that other TiONts–Pc assemblies have been reported for other applications, neither with covalent coupling between two entities, nor with a step-by-step approach.[24,25] Such a coupling was achieved in light of overviews on Click chemistry achieved with porphyrins and

RSC Advances Accepted Manuscript

phthalocyanines,[28] and to hybrid materials incorporating phthalocyanines.[12]

TiONts–Pc nanohybrids **1a-c** were washed with a series of solvents (DMSO/ethanol) and water by ultrafiltration to ensure no free organic material was adsorbed. The coupling of TiONts–X and Pc–Y (to afford conjugate **1a-c**) (Fig. 5) was achieved and thorough characterizations are discussed thereafter (Fig. 4).



Scheme 1. Syntheses of Y-functionalized phthalocyanines **3a-c** (Y = NH_2, COOH, alkyne). (i) 3-hydroxybenzoic acid (1 eq), K_2CO_3 (4 eq), DMF, 25°C, 15 h → **4a**; or (ii) 4-aminophenol (1 eq), K_2CO_3 (2 eq), DMF, 25°C, 15 h → **4b**; or (iii) 4-bromophenol (1 eq), K_2CO_3 (2 eq), DMF, 25°C, 2 h → **4d**; (iv) $Me_3SiC{\equiv}CH$ (2 eq), $Pd(PPh_3)_4$ (0.1 eq), CuI (0.5 eq), NEt_3, 60°C, 2 h → **4a**; (v) $Zn(OAc)_2$ (2 eq), DBU (8 eq), pentanol, 130°C, 15h.

Nanohybrid 1a: XPS analysis showed that the C1s peak decomposes into three different contributions: C–C/C–H (284.5 eV, 62%), C–NH_2 (286.0 eV, 29%), (C=O)–N (287.8 eV, 9%) (Fig. S4).[20] The C–C/C–H components have increased because of the presence of the A_3B–ZnPc aromatics. The N1s peak is shared into three contributions: C–NH_2 (399.7 eV, 54%), C–NH_3^+ (401.3 eV, 31%) and C–N_{Pc} (398.3 eV, 15%). The appearance of a new N1s contribution (C–NPc contribution, 15%) at 398.3 eV is thus attributed to the presence of ZnPc (Fig. S4).[22] TGA indicates 0.13 Pc/nm2 (0.22 µmol/m2) (Fig. S5, Table S2). UV-Visible spectroscopy in DMSO showed the characteristic absorption bands of ZnPc (Q bands: 630 and 679 nm) (Fig. S6-S7). Fluorescence studies show fluorescence emission at 685 nm (Fig. S8).

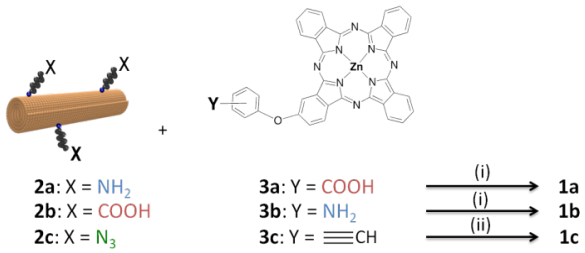


Fig. 4 Coupling TiONts–X **2a-c** and Pc–Y **3a-c** to afford conjugates **1a-c**. (i) EDC/NHS, DMSO, 48h, N_2; (ii) $CuSO_4$, AsNa, 75/25 (v/v) DMSO/H_2O.

Nanohybrid 1b: XPS analysis showed that the C1s peak decomposes into three different contributions: C–C/C–H (284.5 eV, 63%), C=C–N (benzene carbons, 285.9 eV, 27%), (C=O)–OH (288.6 eV, 10%).[20] The C–C/C–H components have increased because of the presence of the A_3B–ZnPc aromatics. The N1s peak is shared into three contributions: C–NH_2 (399.6 eV, 61%), C–NH_3^+ (401.5 eV, 29%) and C–N_{Pc} (398.2 eV, 10%) (Fig. S4).[22] TGA gave 0.1 Pc/nm2 (0.25 µmol/m²) (Fig. S5, Table S2). The appearance of a new N1s contribution at 398.2 eV (attributed to C–NPc contribution) is thus attributed to the presence of ZnPc. UV-Visible spectroscopy into DMSO shows the ZnPc presence (Q bands: 610 and 677 nm) (Fig. S6-S7). Fluorescence studies show fluorescence emission at 687 nm (Fig. S8).

Nanohybrid 1c: ζ-potential measurements (Fig. 4I) indicated an IEP around 8.4 close to the IEP of the previous functionalization stage (TiONts–N_3) but they showed a slight shielding effect due to the grafted A_3B–ZnPc. FTIR showed the disappearance of the azide stretch (Fig. 4II) at 2110 cm^{-1}, which indicates that the reaction with the alkyne occurred, leading to the formation of a resulting triazole linker. XPS analysis (Fig. S9) showed that the C1s peak decomposes into four different contributions: C–C/C–H (284.5 eV, 53%), C–NH_2/C=C–N (286.0 eV, 32%), (C=O)–N (287.5 eV, 11%) and a satellite peak of π→π* transition (291.6 eV, 4%).[20] The C–C/C–H components have increased because of the presence of the A3B–ZnPc aromatics. The N1s peak is shared into three contributions (not shown): C–NH_2 (400.1 eV, 24%), C–NH_3^+ (401.9 eV, 10%) and C–N_{Pc} (398.6 eV, 66%).[22] The appearance of a new N1s contribution (C–NPc contribution) at 398.6 eV is thus attributed to the presence of ZnPc. TGA gave 0.1 Pc/nm² (0.15 µmol/m²) meaning that 1 ZnPc is coupled with 1 PEG–N_3 over 6. UV-Visible spectroscopy in DMSO showed the ZnPc characteristic absorption bands: Q bands (675, 644, and 609 nm), and the Soret band (345 nm). Fluorescence studies show fluorescence emission at 680 nm (Fig. 4IV). Nanohybrids **1a-c** were in the form of small agglomerates (Fig. 4V, S3), which is reminiscent of nanotubes **2a-c**. The surface coverage rates expressed as a function of the available surface groups from the previous step were found to be relevant indicators of the *step-by-step* nanotube-coating. At each stage of the synthesis of conjugate **1**, the coverage rates were the followings determined by TGA: a) 5 OH/nm² (7.8 µmol/m²) on initial bare TiONts; b) 5 NH_2/nm² (8.3 µmol/m²) on TiONts–NH_2 (100% yield), 3.5 COOH/nm² (5.8 µmol/m²) on TiONts–COOH (70% yield); c) 0.6 N_3/nm² (1.0 µmol/m², 12% yield) on TiONts–N_3; d) 0.1 Pc/nm² (0.17 µmol/m²) on TiONts–NH_2/Pc (**1a**) (2.0% yield), 0.1 Pc/nm² (0.17 µmol/m²) on TiONts–COOH/Pc (**1b**) (2.9% yield), and 0.1 Pc/nm² (0.17 µmol/m²) on TiONts–N_3/Pc (**1c**) (17% yield)‡. As a result, it is possible to state that the overall yield was found to be *ca.* 2% grafting on bare TiONts in any case (**1a**, **1b** or **1c**).

Next, spectroscopic studies were carried out to address the imaging capabilities of the Pc probe (*i.e.* fluorescence measurements of ZnPc probe for OI) in the well characterized TiONts–Pc conjugate **1a-c**. Upon excitation of Pc at 600 nm in DMSO solution, a fluorescence emission at 678 nm (**1c**) was observed, which is comparable to the fluorescence emission of the parent ZnPc **3a-c** (not bound to TiONts). These data seem to indicate that aggregation by π-stacking may be limited. Moreover, any possible interaction between TiONt and Pc may not be completely excluded, it may not be extensive because of the steric hindrance provided by the linkers. The hydrophilic character of **1a-c**, may be increased upon either a) tuning down the Pc coverage rate, or b) reacting the remaining azides with

RSC Advances Accepted Manuscript

This journal is © The Royal Society of Chemistry 2012

alkyne-containing PEG. Note that conjugates **1a-c** are putative theranostic agents (*i.e.* a species that can be used to perform imaging and therapy simultaneously).[23] Indeed, not only optical imaging may be achieved from the ZnPc moiety,[9-11] but also it could induce the formation of Reactive Oxygen Species (ROS), by two routes: a) by photodynamic therapy, PDT (from ZnPc probe);[24-26] b) or upon X-Ray irradiation on the nanotube (TiONts).[8] In addition toxicity evaluation of each individual component forming **1a-c** have been reported by us previously[8, 24, 27] leading to the novel nano-objects presented herein.

Experimental

Synthetic procedures

Bare TiONts. Titanate nanotubes (TiONts) were synthesized by a classical hydrothermal method. The precursor is a powder of titanium dioxide (rutile). This powder (440 mg) was added to a NaOH aqueous solution (110 mL, 10 mol.L^{-1}). The mixture was submitted to ultrasounds (15 min, 375 W, Sonics Vibra-Cells) before being transferred to a sealed Teflon reactor. The temperature is set at 155°C during 36 hours and the mixture was stirred by magnetic stirring (120 rpm). The obtained product is washed (dialysis and ultrafiltration on membrane: 30 kDa) down to the pH and the conductivity of deionized water. Finally, the powder was freeze-dried.

TiONts–Pc 1a/1b. TiONts–X (**2a** or **2b**) were subjected to an equivalent mass ratio of Pc–Y (**3a** or **3b**) in the presence of *N*,*N*′-Dicyclohexylcarbodiimide (DCC) and *N*-hydroxysuccinimide (NHS, dissolved into DMSO). The mixture was stirred (60 rpm) in 20 mL of 3:1 THF/water during 48 h followed by evaporation of THF and ultrafiltration against mixture DMSO/water leading to TiONts–Pc 1a or 1b.

TiONts–Pc 1c. TiONts–N_3 were subjected to an equivalent mass ratio of 2-(4-(alkynyl)phenoxy)-phthalocyaninato zinc(II) (alkyne-containing A3B-ZnPc) in the presence of $CuSO_4$ (5.5 molar equivalent) and sodium ascorbate (3.5 molar equivalent) with respect to the alkyne-ZnPc stoichiometry. The suspension was dispersed under ultrasonic treatment (225 W, 15 min, Sonics Vibra-Cells). The mixture was stirred (60 rpm) in 4:1 DMSO/water during 48 h followed by ultrafiltration (mixture DMSO/ethanol) against ethanol leading to TiONts–Pc 1c.

TiONts–NH_2 (2a). Bare TiONts were subjected to 3-aminopropyltriethoxysilane (APTES) in an equivalent mass ratio into 120 mL of a 1:1 ethanol/water mixture. The mixture was submitted to an ultrasonic treatment (225 W, 5 min, Sonics Vibrant-Cells) to afford a good particle dispersion leading to the polysiloxane coverage of individual particles rather than agglomerates. The mixture was then submitted to magnetic stirring (400 rpm) during 48 h. 20 mL of glycerol was then added followed by the evaporation of the ethanol/water mixture under reduced pressure to increase the polysiloxane condensation around TiONts. Finally, glycerol was removed by a mixture acetone/ethanol addition to the TiONts suspension accompanied by a filtration on membrane (regenerate cellulose: 0.45µm). TiONts were finally re-suspended into ultrapure water yielding TiONts–NH_2 and dialyzed one week against ultrapure water (resistivity 18 MΩ).

TiONts–COOH (2b). Bare TiONts were subjected to 6-phosphonohexanoïc acid (PHA) in an equivalent mass ratio into 120 mL of a 1:1 ethanol/water mixture. The mixture was submitted to an ultrasonic treatment (225 W, 5 min, Sonics Vibrant-Cells) to afford good particle dispersion. The mixture was then submitted to magnetic stirring (400 rpm) during 48 h followed by ultrafiltration against ultrapure water (resistivity 18 MΩ) leading to TiONts–COOH.

TiONts–N_3 (2c). TiONts–NH_2 were subjected to an equivalent mass ratio of 32-azido-5-oxo-3,9,12,15,18,21,24,27,30-nonaoxa-6-azadotriacontan-1-oic acid (N_3–PEG_9–COOH) in the presence of *N*-(3-dimethylaminopropyl)-*N*-ethylcarbodiimide hydrochloride (EDC) and *N*-hydroxysuccinimide (NHS, dissolved into DMSO) at 1.0 and 1.1 molar equivalent respectively with respect to the PEG stoichiometry. The mixture was stirred (60 rpm) in 20 mL of 3:1 THF/water during 48 h followed by evaporation of THF and ultrafiltration against ethanol leading to TiONts–N_3.

2-(4-(carboxy)phenoxy)-phthalocyaninato zinc(II) (3a). To a suspension of 3-(3,4-dicyanophenoxy)benzoic acid (0.4 g, 1.51 mmol), phthalonitrile (1.35 g, 10.57 mmol) and zinc acetate dihydrate (663 mg, 3.02 mmol) in octanol (10 mL) was added 1,8-diazabicyclo[5.4.0]undec-7-ene (1.8 mL, 1.84 mmol), then the mixture was heated at 130 °C during 15 hours. The reaction mixture was cooled to room temperature and the blue precipitate was filtered off, washed with 1 M hydrochloric acid (3×20 mL), water (3×20 mL) and methanol (10 mL). The mixture of non-substituted and mono-substituted phthalocyanine was dried under reduce pressure (1.15 g, 43% cyclisation yield).

^{1}H NMR (300 MHz, DMSO, 300 K): 7.78 (m, 2H); 7.85 (d, ^{3}J= 8.0 Hz, 1H); 7.95 (m, 2H); 8.17 (m, 16H), 8.66 (s, 1H); 9.17 (m, 16H); 13.24 (s, 1H). MS MALDI-TOF: m/z= 576.68 $[ZnPc+H]^+$ (calcd for $C_{32}H_{17}N_8Zn^+$: 577.09), 712.82 $[M+H]^+$ (calcd for $C_{39}H_{21}N_8O_3Zn^+$: 713.10). UV-Vis (DMSO): λ_{max} (nm) (ε×103 L.mol^{-1}.cm^{-1})= 347 (45.5), 608 (26.3), 673 (168.2).

2-(4-(amino)phenoxy)-phthalocyaninato zinc(II) (3b). To a suspension of 4-(4-(amino)phenoxy)phthalonitrile (0.5 g, 2.13 mmol), phthalonitrile (1.9 g, 14.88 mmol) and zinc acetate dihydrate (933 mg, 4.25 mmol) in octanol (10 mL) was added DBU (2.55 mL, 2.59 mmol), then the mixture was heated at 130 °C during 15 hours. The reaction mixture was cooled to room temperature and the blue precipitate was filtered off, washed with 1 M hydrochloric acid (3×30 mL), water (3×30 mL), methanol (20 mL), then subsequently washed with dichloromethane for 12 h in a Soxhlet extractor. The blue-green solid was dried under reduced pressure to afford the mixture of non-substituted and mono-substituted phthalocyanine (950 mg, 35 % cyclisation yield).

^{1}H NMR (300 MHz, DMSO-d_6, 298 K): δ (ppm)= 6.86 (d, J= 8.7 Hz, 2H); 7.24 (d, J= 8.7 Hz, 2H); 7.91 (m, 1H), 8.22 (m, 18H); 8.57 (s, 1H); 9.17 (m, 1H); 9.30 (m, 18H). MS MALDI-TOF: m/z= 576.68 $[ZnPc+H]^+$ (calcd for $C_{32}H_{17}N_8Zn^+$: 577.09), 683.82 $[M+H]^+$ (calcd for $C_{38}H_{22}N_9OZn^+$: 684.13). UV-Vis

RSC Advances Accepted Manuscript

(DMSO): λ_{max} (nm) (ε×103 L.mol^{-1}.cm^{-1}) = 347 (40.4), 608 (23.6), 674 (146.7).

2-(4-(alkynyl)phenoxy)-phthalocyaninato zinc(II) (3c). A suspension of 4-(4-((trimethylsilyl)ethynyl)phenoxy)phthalonitrile (3) (0.4 g, 1.26 mmol), phthalonitrile (1.13 g, 8.82 mmol), zinc acetate dihydrate (553 mg, 2.52 mmol), in octanol (10 mL) and 1,8-diazabicyclo[5.4.0]undec-7-ene (1.5 mL, 10.1 mmol) was heated at 130 °C during 2 hours. Then the reaction mixture was cooled to 21 °C and the blue precipitate was filtered off, washed with 1 M hydrochloric acid (3×20 mL), water (3×20 mL) and methanol (10 mL), then subsequently washed with dichloromethane for 12 h in a Soxhlet extractor. The blue solid was dried under reduced pressure to afford the mixture of non-substituted A_4-ZnPc and mono-substituted A_3B-ZnPc phthalocyanine (where A_4 stands for four unsubstituted isoindoles of the ZnPc and A_3 for three unsubstituted isoindoles, B stands for the alkyne-containing isoindole; 400 mg of mixture, 25 % cyclisation yield).

^{1}H NMR (300 MHz, DMSO-d_6, 298 K): δ (ppm) = 4.28 (s, 1H); 7.55 (d, J= 8.0 Hz, 2H); 7.67 (d, J= 8.1 Hz, 1H); 7.81 (d, J= 8. 0 Hz, 2H), 8.1 (m, 16H); 8.3 (s, 1H); 8.77 (d, J= 8.1 Hz, 1H); 8.90 (m, 2H); 8.99 (m, 14H). MALDI-TOF MS: m/z= 576.23 $[ZnPc+H]^+$ (calcd for $C_{32}H_{17}N_8Zn^+$: 577.09), 692.5 $[M+H]^+$ (calcd for $C_{40}H_{21}N_8OZn^+$: 693.11). UV-Vis (DMSO), λ_{max} (nm) (.103 ε): 344 (41.3), 603 (21.3), 640 (19.5), 667 (142.2).

4-(carboxylato)phenoxy)phthalonitrile (4a). This compound was synthesized by adapting the method described by Erdem et al.[29] and modified as follows (adapted for this regioisomer and improvements are T conditions, solvent, and yields). A suspension of 4-nitro-phthalonitrile (3 g, 17.3 mmol), 3-hydroxybenzoic acid (2.39 g, 17.3 mmol) and potassium carbonate (9.56 g, 75.2 mmol) were stirred in DMF (30 mL) at room temperature during 15 hours. After addition of 100 mL of 1 M hydrochloric acid, the resulting precipitate was filtered off and washed with water (3×50 mL). The solid obtain was dry under reduce pressure (3.97 g, 98 %).

^{1}H NMR (300 MHz, DMSO-d_6, 300 K): δ (ppm)= 7.45 (m, 2H); 7.62 (m, 2H); 7.85 (m, 2H); 8.10 (d, ^{3}J= 8.7 Hz, 1H); 13.23 (s broad, 1H). ^{13}C NMR (75 MHz, DMSO-d_6, 300 K): δ (ppm)= 108.7; 115.3; 115.8; 116.8; 120.6; 122.4; 123.0; 124.7; 126.4; 131.0; 133.4; 136.3; 154.0; 160.6; 166.3. MS ESI-Q: m/z= 262.83 $[M-H]^-$ (calcd for $C_{18}H_9N_4O_2^+$: 263.03).

4-(amino)phenoxy)phthalonitrile (4b). This compound was synthesized accrding to a method described by D'Souza et al.[30] and modified as follows (improvements are RT conditions, solvent, and yields). A mixture of 4-nitro-phthalonitrile (3 g, 17.3 mmol), 4-aminophenol (1.89 g, 17.8 mmol) and potassium carbonate (4.78 g, 34.6 mmol) was stirred in DMF (30 mL) at room temperature during 15 hours. After addition of 60 mL of water, the resulting precipitate was filtered off and washed with water (3×20 mL). The pale yellow solid obtain was dry under reduce pressure to afford compound 4 (3.8 g, 94 %). ^{1}H NMR (300 MHz, DMSO-d_6, 300 K): δ (ppm)= 5.18 (s, 2H); 6.64 (d, ^{3}J= 8.9 Hz, 2H); 6.85 (d, ^{3}J= 8.9 Hz, 2H); 7.25 (dd, ^{3}J= 8.8 Hz, ^{4}J= 2.6 Hz, 1H); 7,6 (d, ^{4}J= 2.6 Hz, 1H); 8.02 (d, ^{3}J= 8.8 Hz, 1H). ^{13}C NMR (75 MHz, DMSO-d_6, 300 K): δ (ppm)= 106.9; 114.9; 115.4; 116.0; 116.4; 120.7; 121.3; 121.4; 136.1; 143.0; 146.9; 162.2. MS ESI-Q: m/z= 233.87 $[M-H]^-$ (calcd for $C_{14}H_8N_3O$: 234.07).

4-(4-((trimethylsilyl)ethynyl)phenoxy)phthalonitrile (4c). It was synthesized upon modification of the original procedure described by us[15] that led to a significant improvement in yields. A solution of trimethylsilylacetylene (328 mg, 3.34 mmol) in triethylamine (20 mL) was added to a mixture of de 4-(4-bromophenoxy)phthalonitrile **(4)** (0.5 g, 1.67 mmol), palladium (tetrakis-triphenyl)phosphine (193 mg, 0.167 mmol) and copper iodide (159 mg, 0.835 mmol) under argon atmosphere. The mixture was heated at 60 °C during 2 hours. After addition of dichloromethane (30 mL), the organic layer was washed with brine (3×30 mL), saturated NH_4Cl solution (3×30 mL), water (30 mL) and dried with $MgSO_4$. The solvent was evaporated and the resulting oil was purified by column chromatography (hexane/AcOEt, 80:20) to obtain 4-(4-((trimethylsilyl)ethynyl)phenoxy)phthalonitrile **(3)** as a white powder (420 mg, 81%).

^{1}H NMR (300 MHz, $CDCl_3$, 300 K): δ (ppm) = 0.11 (s, 9H, $Si(CH_3)_3$); 6.85 (d, ^{3}J= 8.7 Hz, 2H, H_5); 7.07 (dd, ^{3}J= 8.5 Hz, ^{4}J= 2.6 Hz, 1H, H_2); 7.13 (d, ^{4}J= 2.6 Hz, 1H, H_1); 7.39 (d, ^{3}J= 8.6 Hz, 2H, H_4); 7.57 (d, ^{3}J= 8.7 Hz, 1H, H_3). ^{13}C NMR (75 MHz, $CDCl_3$, 300 K): δ (ppm) = 5.1; 100.0; 110.0; 114.1; 120.6; 121.1; 122.1; 125.5; 124.7; 128; 128.5; 139.2; 141.6; 159.6; 165.4. MS ESI-Q: m/z calc.= 339.3 $[M+Na]^+$ (calcd. for $C_{18}H_9N_4O_2^+$: 339.09).

4-(4-bromophenoxy)phthalonitrile (4d). A mixture of 4-nitro-phthalonitrile (1 g, 5.8 mmol), 3-bromophenol (1 g, 5.8 mmol) and potassium carbonate (1.6 g, 11.6 mmol) was stirred in DMF (20 mL) at room temperature during 2 hours. After addition of 20 mL of water, the resulting precipitate was filtered off and washed with water (3×10 mL). The white-pink solid obtain was dry under reduce pressure to afford compound 4 (1.73 g, 95%).

^{1}H NMR (300 MHz, DMSO-d6, 298 K): δ (ppm)= 7.31 (d, ^{3}J= 8.8 Hz, 2H, H_5); 7.58 (dd, ^{3}J= 8.6 Hz, ^{4}J= 2.6 Hz, 1H, H_2); 7,63 (d, ^{4}J= 2.6 Hz, 1H, H_1); 7.92 (d, ^{3}J= 8.8 Hz, 2H, H_4); 8,08 (d, ^{3}J= 8.6 Hz, 1H, H_3).

Materials and methods

Chemicals. Chemicals used in this study are from various providers: Acros Organics [3-hydroxybenzoïc acid (99%, ref. 120981000), 4-aminophenol (97 %, ref. 104272500), 4-bromophenol (97 %, ref. 304411000), copper iodide (99.9 %, ref. 201500050), 1,8-diazabicyclo[5.4.0]undec-7-ene (98 %, ref. 160615000), 1,2-dicyanobenzene (98 %, ref. 174012500), dimethylsulfoxide (> 99.7%, ref. 34844), octanol (99 %, ref. 150630020), tetrakis(triphenylphosphine) palladium (99 %, ref. 202380010), triethylamine (99 %, ref. 157910010), zinc acetate dihydrate (98 %, ref. 207640010)], Carlo Erba [potassium carbonate (pure, 359809)], Fisher Chemicals [THF (BHT-stabilized, ref. T/0701/21), Copper sulfate (II) CuSO4.5H2O (98%, ref. C/8520/60)], Fluka [*N*-(3-dimethylaminopropyl)-*N'*-ethylcarbodiimide hydrochloride (≥ 98%, ref. 03450)], IRIS

RSC Advances Accepted Manuscript

This journal is © The Royal Society of Chemistry 2012

Biotech [32-azido-5-oxo-3,9,12,15,18,21,24,27,30-nonaoxa-6-azadotriacontan-1-oic acid (554.59 $g.mol^{-1}$, ref. PEG2015)], Sigma-Aldrich [3-aminopropyltriethoxysilane (≥ 98%, ref. A3648), dimethylformamide (>99%, ref. 15440), ethynyltrimethyl-silane (98 %, ref. 101061688), 6-phosphohexanoic acid (97 %, 693839) *N*,*N*′-Dicyclohexylcarbodiimide (99%, D80002), sodium L-ascorbate (98%, ref. A7631), *N*-hydroxysuccinimide (98%, ref. 130672), sodium hydroxide pellets (≥ 98%, ref. S5881) and TCI [4-nitro-1,2-dicyanobenzene (TCI, >98 %, ref. N0524)] and Tioxide® [titanium dioxide rutile powder]. Chemicals were used as received without any further purification when no otherwise stated.

Characterizations. Chromatography: compounds **4a – 4d** were purified on column chromatography using silica gel (60A, SDS) and a specific mixture of solvents as described in section 2. Zeta Potential: Zeta potential measurements were performed on a Zeta-Nanosizer (Malvern) into 10-2 M NaCl solutions. ESI-Q MS (ElectroSpray Ionisation-Quadripole Mass Spectroscopy): measurements were performed on LTQ Orbitrap XL (THERMO) coupled to HPLC Ultimate 3000 (DIONEX); 1 mg compound into 1 mL of appropriate solvent, diluted 100 times with methanol. Spectrofluorimetry: Fluorolog Jobin Yvon Horiba equipped with a Xe source. Fluorescence spectra for free ZnPc and conjugate **1a-c** were recorded in THF, ethanol or dimethylsulfoxyde. Excitation was performed at 600 nm and emission spectrums were recorded for an absorbance at excitation wavelength between 0.03 and 0.07. Fourier Transformed InfraRed spectroscopy (FTIR): measurements were performed on a FTIR Bruker Vertex 70v spectrometer; samples were analyzed on KBr pellets, which were prepared as follows: KBr powder (150 mg) and powder sample (2 mg) were mixed and pressed. TiONts FTIR spectra were recorded and processed by OPUS software: depending on their nature, samples were analyzed as powders into dried KBr or as liquids through an ATR device. MALDI-TOF MS (Matrix-Assisted Laser Desorption/Ionization - Time of Flight Mass Spectroscopy). Measurements were performed on Ultraflex II LRF 2000 (BRUKER); matrix used: dithranol; 1 mg compound into 1 mL DMSO. NMR spectroscopy: Measurements were performed on a Bruker Dalton X, at 300 MHz (^{1}H), or 75 MHz (^{13}C) in $CDCl_3$ or DMSO-d_6 (*ca*. 5-10 mg/400 µL (^{1}H-NMR), and twice as much for ^{13}C-NMR). Chemical shifts are expressed in ppm relative to TMS (residual chloroform from deuterated chloroform chemical shift was set at 7.26 ppm, and residual dimethylsulfoxide from deuterated dimethylsufoxyde chemichal shift at 2.50 ppm). Surface area measurement: measurements were performed using a BELSORP-mini apparatus with N_2 gas adsorption. The BET method has been used in the calculation of surface area values (S_{BET}) from the isotherm of nitrogen adsorption. TEM: Transmission Electron Microscopy images were obtained from a JEOL JEM 2100 LaB_6 operating at 200 kV (point resolution 2.5 Å). The copper grids were dipped in dilute suspension of samples in ethanol and naturally dried. ThermoGravimetric Analysis (TGA): desorption of TiONts and decomposition of the organic compounds were studied by thermogravimetry (TGA DISCOVERY). This symmetric thermobalance is able to measure weight variations of 0.1 µg. Heating rate was 5°C up to 800°C N_2 (25 mL/min). Sample weight was 5-10 mg. UV-Visible spectroscopy: ZnPc, TiONts and TiONts–Pc **1a-1b** spectra were obtained on a Shimadzu UV-2550 spectrophotometer. Free phthalocyanines **3a-3b** and TiONts–Pc conjugate **1a-c** spectra were recorded in DMSO in glass cuvettes 1x1x3 cm (1 cm path). Other samples were measured as particle suspensions into ultrapure water (resistivity 18 MΩ) when no otherwise stated. XPS: X-ray Photoelectron Spectroscopy data were recorded on a PHI Versaprobe 5000 device and Al–K_α monochromatic radiation (1486.6 eV, 50 W with a 200-µm-diameter spot size) was used as X-ray source. Pass energy is 200 eV for spectra and 60 eV for windows (quantifications and curve fitting are obtained from windows acquisitions). Powder samples were prepared by pressing the sample powder on an indium sheet. Neutralization was used to minimize charge effects and the adventitious carbon C1s peak at 284.5 eV was used as the reference. The pressure in analysis chamber during acquisition is around 8.10^{-8} Pa. Photoemission peak areas were calculated after background subtraction using a Shirley routine and all concentration calculations were done with Multipack software. Windows were decomposed into components by fitting with Gaussian (70%)-Lorentzien (30%) peaks. In the fitting procedure, Full-Widths at Half-Maximum (FWHMs) were set with Casa XPS software.

Conclusions

This work presented the successful functionalization *step-by-step* of TiONts up to three times using classical reactions of organic synthesis (silanization, acylation, cycloaddition) with the functional groups or molecules found at the TiONts surface: hydroxyl groups (bare TiONts), amine or carboxylic acid groups (first stage coating), azide groups (second stage coating), and phthalocyanines (second stage coating in **1a-b**, third stage coating in **1c**), respectively.

The coupling methodology used, *i.e.* whether amide bond formation between TiONts–NH_2 **2a** and acid–Pc **3a**, or TiONts–COOH **2b** and amino–Pc **3b** (leading to conjugates **1a-b**) or click chemistry[28] between TiONts–N_3 and alkyne-Pc proceeded equally well. However, the resulting conjugates **1a** and **1b** were not stable enough in water, whereas **1c** was found to be reasonably more stable (Fig. S11). This may be because of the PEG-linker in **1c**. Moreover, a satisfactory point in **1c** is that click chemistry proceeds well, and only required water-soluble and easily removable copper catalyst and reducing agent, unlike amide bond formation in **1a-b** (peptide coupling requires EDC and NHS). Indeed, the synthesis of **1c** did not require the use of extra organic reagents, which is an asset for subsequent purification purposes. These reactions proceeded smoothly and each TiONts end-products were well identified and thoroughly characterized by an extensive number of spectroscopic techniques *step-by-step*. Based on preliminary

RSC Advances Accepted Manuscript

data (fluorescence measurements), we are confident on the relevant nature of **1c**.

Acknowledgements

JB, RAD thank the Burgundy Regional Council, CRB (FABER Programs), RAD thanks CNRS for Chaire d'Excellence; JB, YB thank CRB (JCE, FABER grants respectively). This work was supported by 3MIM agreement (CNRS, uB and CRB), and labeled by the PharmImage® consortium.

Notes and references

[a] Laboratoire Interdisciplinaire Carnot de Bourgogne (ICB), UMR 6303 CNRS-Université de Bourgogne, BP 47870, F-21078, Dijon Cedex, France; E-mail: Nadine.Millot@u-bourgogne.fr

[b] Institut de Chimie Moléculaire de l'Université de Bourgogne (ICMUB), UMR 6302 CNRS-Université de Bourgogne, BP 47870, F-21078, Dijon Cedex, France; E-mail: Richard.Decreau@u-bourgogne.fr

† Footnotes should appear here. These might include comments relevant to but not central to the matter under discussion, limited experimental and spectral data, and crystallographic data.

Electronic Supplementary Information (ESI) available: [details of any supplementary information available should be included here]. See DOI: 10.1039/b000000x/

1. S. L. Pimlott and A. Sutherland, *Chem. Soc. Rev.*, 2011, **40**, 149-162.
2. T. J. Wadas, E. H. Wong, G. R. Weisman and C. J. Anderson, *Chem. Rev.*, 2010, **110**, 2858-2902.
3. C. Rümenapp, B. Gleich and A. Haase, *Pharm. Res.*, 2012, **29**, 1165-1179.
4. V. J. Pansare, S. Hejazi, W. J. Faenza and R. K. Prud'homme, *Chem. Mater.*, 2012, **24**, 812-827.
5. Z. Liu, S. M. Tabakman, Z. Chen and H. Dai, *Nat. Protocols*, 2009, **4**, 1372-1381.
6. A.-L. Papa, L. Maurizi, D. Vandroux, P. Walker and N. Millot, *J. Phys. Chem. C*, 2011, **115**, 19012-19017.
7. A. L. Papa, L. Dumont, D. Vandroux and N. Millot, *Nanotoxicology*, 2013, **7**, 1131-1142.
8. C. Mirjolet, A. L. Papa, G. Créhange, O. Raguin, C. Seignez, C. Paul, G. Truc, P. Maingon and N. Millot, *Radiother. Oncol.*, 2013, **108**, 136-142.
9. N. Sekkat, H. v. d. Bergh, T. Nyokong and N. Lange, *Molecules*, 2011, **17**, 98-144.
10. E. Ben-Hur and W.-S. Chan, in *Porphyrin Handbook*, eds. K. M. Kadish, K. M. Smith and R. Guilard, Elsevier Science, USA, 2003, vol. 19, pp. 1-35.
11. L. D. Lavis and R. T. Raines, *ACS Chemical Biology*, 2008, **3**, 142-155.
12. M. Bouvet, P. Gaudillat and J.-M. Suisse, *J. Porphyrins Phthalocyanines*, 2013, **17**, 913-919.
13. L. Maurizi, F. Bouyer, J. Paris, F. Demoisson, L. Saviot and N. Millot, *Chem. Commun.*, 2011, **47**, 11706-11708.
14. L. Maurizi, H. Bisht, F. Bouyer and N. Millot, *Langmuir*, 2009, **25**, 8857-8859.
15. J. Boudon, J. Paris, Y. Bernhard, E. Popova, R. A. Decreau and N. Millot, *Chem. Commun.*, 2013, **49**, 7394-7396.
16. R. A. Decréau, J. P. Collman, Y. Yang, Y. Yan and N. K. Devaraj, *J. Org. Chem.*, 2007, **72**, 2794-2802.
17. J. P. Collman, N. K. Devaraj, R. A. Decréau, Y. Yang, Y.-L. Yan, W. Ebina, T. A. Eberspacher and C. E. D. Chidsey, *Science*, 2007, **315**, 1565-1568.
18. J. P. Collman, R. A. Decréau, H. Lin, A. Hosseini, Y. Yang, A. Dey and T. A. Eberspacher, *Proc. Natl. Acad. Sci.*, 2009, **106**, 7320-7323.
19. A.-L. Papa, N. Millot, L. Saviot, R. Chassagnon and O. Heintz, *J. Phys. Chem. C*, 2009, **113**, 12682-12689.
20. P. G. Rouxhet and M. J. Genet, *Surf. Interface Anal.*, 2011, **43**, 1453-1470.
21. J. Böhmler, L. Ploux, V. Ball, K. Anselme and A. Ponche, *J. Phys. Chem. C*, 2011, **115**, 11102-11111.
22. L. Zhang, H. Peisert, I. Biswas, M. Knupfer, D. Batchelor and T. Chassé, *Surf. Sci.*, 2005, **596**, 98-107.
23. S. S. Kelkar and T. M. Reineke, *Bioconjugate Chem.*, 2011, **22**, 1879-1903.
24. R. A. Decréau, M. J. Richard, P. Verrando, M. Chanon and M. Julliard, *J. Photochem. Photobiol. B: Biol.*, 1999, **48**, 48-56.
25. R. A. Decréau, A. Viola, M. J. Richard, A. Jeunetan and M. Julliard, *J. Porphyrins Phthalocyanines*, 1998, **02**, 405-414.
26. F. Lv, X. He, l. Lu, L. Wu and T. Liu, *J. Porphyrins Phthalocyanines*, 2012, **16**, 77-84.
27. R. A. Decréau, M.-J. Richard and M. Julliard, *J. Porphyrins Phthalocyanines*, 2001, **05**, 390-396.
28. F. Dumoulin and V. Ahsen, *J. Porphyrins Phthalocyanines*, 2011, **15**, 481-504.
29. S. S. Erdem, I. V. Nesterova, S. A. Soper, R. P. Hammer, *J. Org. Chem.* 2009, **74**, 9280-9286.
30. S. D'Souza, E. Antunes, T. Nyokong, *Inorg. Chim. Acta,* 2011, **367**, 173-181

RSC Advances Accepted Manuscript

 This journal is © The Royal Society of Chemistry 2012